Advanced Composite Materials
Publication details, including instructions for authors and subscription information:
http://www.tandfonline.com/loi/tacm20

Broadband radar absorbing structures of carbon nanocomposites

Jin-Bong Kim [a]

[a] Composite Materials Laboratory, Korea Institute of Materials Science, 797 Changwondaero, Seongsangu, Changwon, Gyeongnam, 642-831, South Korea

Version of record first published: 18 Oct 2012.

To cite this article: Jin-Bong Kim (2012): Broadband radar absorbing structures of carbon nanocomposites, Advanced Composite Materials, 21:4, 333-344

To link to this article: http://dx.doi.org/10.1080/09243046.2012.736350

Advanced Composite Materials
Vol. 21, No. 4, August 2012, 333–344

Taylor & Francis
Taylor & Francis Group

Broadband radar absorbing structures of carbon nanocomposites

Jin-Bong Kim*

Composite Materials Laboratory, Korea Institute of Materials Science, 797 Changwondaero, Seongsangu, Changwon, Gyeongnam 642-831, South Korea

(*Received 22 October 2011; accepted 21 May 2012*)

In this paper, we present double-layer radar absorbing structures composed of E-glass fabric/epoxy composite laminates that are optimally designed to have a broad bandwidth in the X-band. The first layer is a pure E-glass fabric/epoxy composite laminate and the second layer is a carbon nanocomposite laminate. Composite prepregs of carbon nanomaterials containing carbon black (CB), carbon nanotubes (CNT), and carbon nanofibers (CNF) were used. Numerical models of the complex permittivity of carbon nanocomposites were incorporated into the design process to determine the optimal thicknesses of both the first and the second layers and the optimal filler content of the second layer. By changing the locations of the two peaks in the frequency domain, various radar absorbing structures with different absorbing performances were designed. At the same time, the influence of the electromagnetic characteristics of each carbon nanomaterial on the thickness and the absorbing performance was investigated. The thickness and 10-dB bandwidth were 4.680 mm and 7.5 GHz for CB-composites, 4.090 mm and 7.7 GHz for CNF-composites, and 4.277 mm and 7.4 GHz for CNT-composites, respectively. The broad bandwidth of the CNF-composite as compared to its thickness was attributed to its high dielectric constant as compared to the lossy term of its complex permittivity.

Keywords: carbon; nanocomposites; microwave absorber; electrical properties; optimal design

1. Introduction

Since the World War II, the radar system has been the biggest threat to aircraft. Microwave, or radar, absorbing technology has been used as a potential method to mitigate this threat [1,2]. In commercial fields, microwave absorbing technology is used as a solution to the radar interference between large objects and air traffic control radars or military surveillance radars. For example, it has been reported that the microwave, or radar, absorbing technology is necessary for manufacturers of composite blades, especially those having a length of over 40 m, for wind turbine systems [3]. Moreover, recent advancements in electromagnetic applications such as electric automobiles are increasing the demand for microwave, or radar, absorbing technology in various commercial fields.

Microwave absorbers are usually applied on the outer surfaces of structures with complex curvatures. Therefore, in addition to the absorbing performance, properties such as the convenience of applying on a wide range of surfaces and a resistance to harmful environments are essential for a good absorber. For these reasons, composite laminate is an attractive material

*Email: jbkim@kims.re.kr

ISSN 0924-3046 print/ISSN 1568-5519 online

http://dx.doi.org/10.1080/09243046.2012.736350
http://www.tandfonline.com

for radar absorbing technology. Recently, many studies on E-glass fiber-reinforced polymer matrix composites have been reported. These composites have a high structural performance as well as the capability to act as a microwave absorber when lossy nanofillers are added to the polymer matrix [4–9]. This composite has drawn attention not only for its structural performance, but also for its merits in the manufacturing process. In the manufacturing process, the epoxy resin for the composite prepreg can be diluted with acetone resulting in a low viscosity resin that allows a very high concentration of nanofillers. Acetone evaporates readily in the drying process of the prepreg. Moreover, the fiber-reinforcement can prevent the sinkage of agglomerations of nanofillers in the low viscosity polymer resin at high curing temperatures, which can cause the composite properties to vary [10]. To construct a material with a broad absorbing bandwidth, the inherent layered structure of the composite laminate is very useful to form a multi-layer (including two-layer) Dallenbach-type radar absorbing structure (RAS) over a large area with a relatively uniform thickness [4,6].

The broad bandwidth of the multi-layer RAS is achieved by multiple peaks in the frequency domain, of which the number is in one-to-one ratio with the number of layers. The absorbing performance is very dependent on the locations of the peaks. From the early 1990s, many numerical schemes were studied as optimization methods for multi-layer absorbers. These studies showed that the peaks could be efficiently placed in the frequency domain by optimizing the thickness, complex permittivity, and complex permeability of each layer [11–16]. However, it must be pointed that even though the optimization results were excellent, it is not easy to obtain real materials of which the four electric properties, including the real and imaginary parts of the complex permittivity and complex permeability, fully agree with the optimized ones in all frequency ranges of interest. For this reason, some of the previous studies adopted various theoretical material models with assumed parametric constants in their optimization process without any guarantee of how to obtain those materials [12,14].

Microwave absorbers can be categorized into magnetic and dielectric absorbers according to their lossy fillers. Most magnetic fillers are very heavy and need to be mixed with a high mixing ratio. In this study, we deal with only carbon nanofillers as the lossy materials, including carbon black (CB), carbon nanofibers (CNF), and multi-walled carbon nanotubes (CNT). It was reported that the electrical property of carbon nanocomposites is dependent on the selection of the carbon nanofiller [9]. We investigated the influence of the selection of the carbon nanofiller on the characteristics of the broadband absorbers by performing an optimization of the design process for the double-layer absorber composed of E-glass fabric/epoxy composite laminates with the different kinds of carbon nanofillers. Recently, Kim et al. [10] measured the complex permittivity of E-glass fabric/epoxy composite laminates containing CB, CNF, and multi-walled CNT, and proposed a semi-empirical model that can describe the complex permittivity of the composites as a function of the frequency and filler content. In this study, the filler contents and the thicknesses of the composites are used directly as optimization variables by adopting the semi-empirical model proposed by Kim et al. [10] in the optimizing process. The absorbers containing CB-, CNF-, and CNT- composites were fabricated and the influence of the characteristics of the complex permittivity of each composite on the performance of absorbers was verified.

2. Complex permittivity model for composites

The carbon nanomaterials used in this study are carbon black (HG-1P of LINZI HUAGUANG Chemical Ind., China), carbon nanofibers (PYROGRAH-III (PR-19-XT-LHT) of APPLIED SCIENCE Inc., USA), and multi-walled carbon nanotubes (CM-95 of HANWHA NANOTECH Co. Ltd., Korea). Table 1 and Figure 1 show the characteristics and images of

Table 1. Dimensions of carbon nanomaterials [10].

Material	Diameter	Length
CB	0.3 μm (0.025 μm powder)[a]	–
CNT	0.01–0.015 μm[a]	10–20 μm[a]
CNF	0.15 μm[a]	10–30 μm[a]

[a]Values obtained from manufacturers.

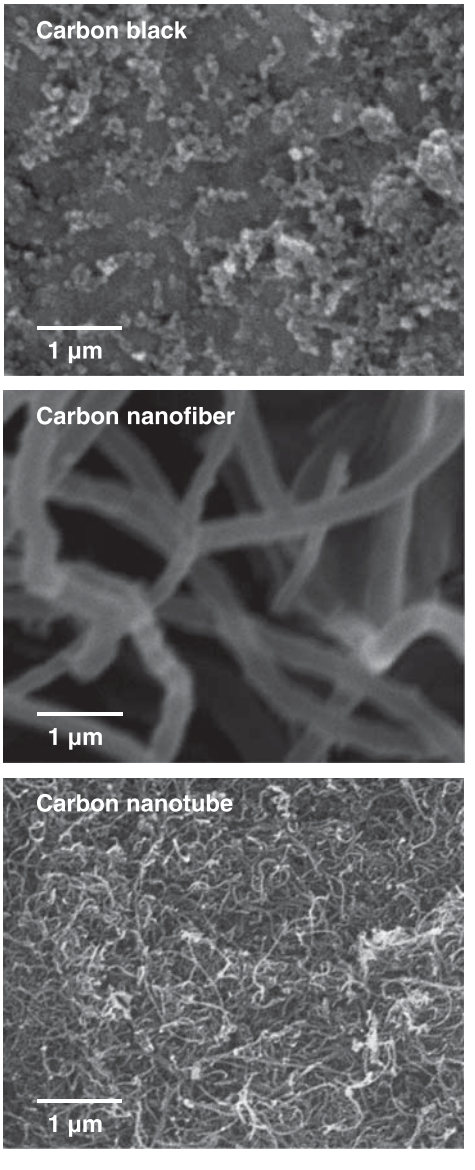

Figure 1. Scanning electron images of CB, CNF, and multi-walled CNT [10].

the carbon nanomaterials, respectively. Composite prepregs were manufactured by coating the epoxy resin mixture and each carbon nanomaterial onto the E-glass fabric mat (#110 EPC glass mat supplied by HANKUK Fiber Co. Korea). The fabric mat was a plain weave type with fiber counts of 60 and 57 yarns/in in the warp and fill directions, respectively. The fiber aerial weight was 107 g/m^2. The laminates in Figure 2 were fabricated at 80 °C for 30 min and 120 °C for over 2 h at a pressure of 6 atm in an autoclave. The nominal thickness of the prepregs was approximately 0.114 ± 0.02 mm and the resin content (R/C) of a ply in the cured laminates was approximately 43 wt.% [10].

Complex permittivity, an AC electrical property, is expressed as $\varepsilon_r = \varepsilon'_r - j\varepsilon''_r$, where ε'_r is the dielectric constant and ε''_r is a lossy term that is related to the AC electric conductivity, σ_{AC}, of the material. The relationship between ε''_r and σ_{AC} is $\sigma_{AC} = 2\pi f \varepsilon_0 \varepsilon''_r$, where f is the wave frequency and ε_0 is the absolute permittivity of air (or the vacuum). The complex permittivity, ε_r, can be expressed as follows:

$$\varepsilon_r = \varepsilon'_r - \left(\frac{j\sigma_{AC}}{2\pi f \varepsilon_0}\right) \tag{1}$$

The pure E-glass/epoxy composite laminate is an insulating material and its complex permittivity is 4.7 – j0.16 which is almost constant within the frequency region we are interested in.

For carbon nanocomposites, Kim et al. [10] proposed that for filler contents, p [wt.%], greater than the percolation threshold, p_c, in a frequency range above the critical frequency, f_ξ, over which the AC electrical conductivity, σ_{AC}, increases proportionally to the frequency, σ_{AC} and ε'_r can be expressed as follows:

$$\sigma_{AC} = K_1 f^x + K_2, \tag{2}$$

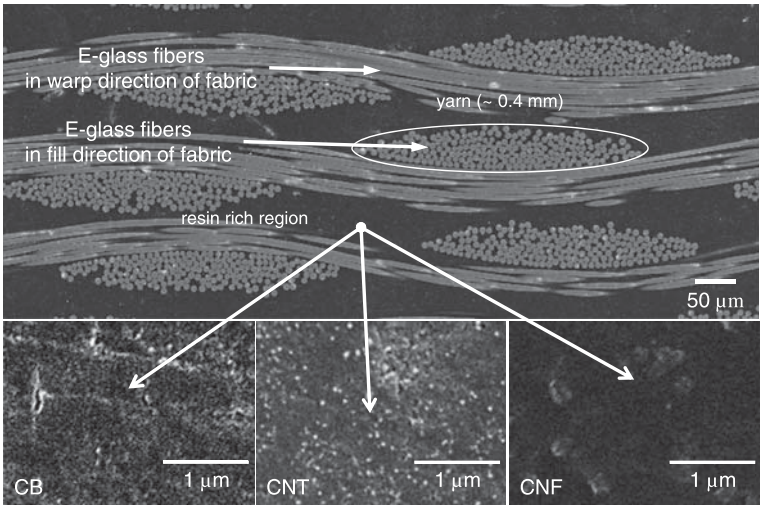

Figure 2. Cross-sectional scanning electron images of E-glass fiber-reinforced carbon nanocomposite laminates [10].

$$\varepsilon_{\mathrm{r}}' = K_3 f^{-y} + K_4 \tag{3}$$

In Equations (2) and (3), K_i can be defined as follows:

$$K_i = a_i(p - p_{\mathrm{c}})^{b_i} + \mathrm{c}_i; \quad i = 1, 2, 3 \text{ and } 4 \tag{4}$$

The coefficients a_i, b_i, and c_i can be calculated from the measured complex permittivity of CB-, CNF-, and CNT-composites, respectively. From Equations (1)–(4), it can be seen that the complex permittivity is dependent on both the filler content and the wave frequency.

3. Optimal design of absorbers

3.1. Reflection of multi-layer absorbers

The governing equation of a multi-layer absorber can be achieved using the transmission line method. Figure 3 is a schematic drawing of a double-layer absorber. The reflection coefficient, R, of the model can be expressed as follows:

$$R = \frac{\eta_{\mathrm{in}}^{(0)} - \eta_0}{\eta_{\mathrm{in}}^{(0)} + \eta_0}, \quad \text{where } \eta_{\mathrm{in}}^{(i-1)} = \eta_i \frac{\eta_{\mathrm{in}}^{(i)} + \eta_i \tanh(\gamma_i d_i)}{\eta_i + \eta_{\mathrm{in}}^{(i)} \tanh(\gamma_i d_i)} \quad \text{and } \eta_{N+1} = 0 \tag{5}$$

In Equation (5), the characteristic impedance, η_i, and the propagation constant, γ_i, are functions of the permittivity, $\varepsilon_{\mathrm{r,i}}$, and permeability, $\mu_{\mathrm{r,i}}$, of the media through which the electromagnetic wave travels. For dielectric absorbers, the permeability is unity. Therefore, the characteristic impedance and propagation constant can be written as $\eta_i = \sqrt{1/\varepsilon_{\mathrm{r},i}}$ and $\gamma_i = j2\pi f\sqrt{\varepsilon_{\mathrm{r},i}}/c$, respectively, where c is the speed of light in air. The input impedance in the $(i-1)$th layer, $\eta_{\mathrm{in}}^{(i-1)}$, can be calculated recursively from the ith properties, where the characteristic impedance of air, η_0, is unity. In this study, the double-layer radar absorbing composite laminate was designed to be composed of a pure E-glass/epoxys laminate (coded as [NON]) first layer and a carbon nanocomposite laminate (coded as [CB] for CB-composites, [CNF] for CNF-composites, and [CNT] for CNT-composites) second layer.

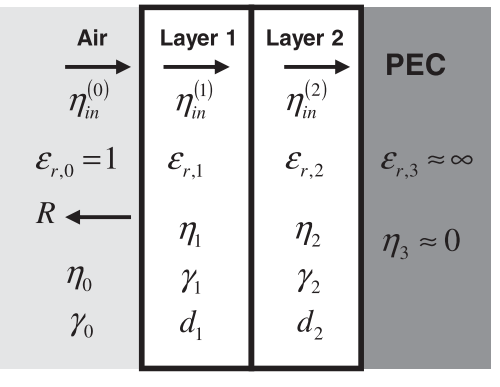

Figure 3. Schematic representation of double-layer absorber.

3.2. Optimization of double-layer absorbers

In general optimization processes for double-layer absorbers composed of dielectric materials, the optimization variables are the thicknesses and the real and imaginary parts of the complex permittivity of each layer. For the optimization of the double-layer absorbers in our study, we applied the complex permittivity model proposed by Kim et al. [10] in the second layer of Equation (5). As a result, the variables in the optimization process are the thicknesses of the first and second layers and the filler content of the second layer. The optimization was performed using a genetic algorithm [17] that has already been successfully used in the previous research by Michielssen et al. [12] and Weile et al. [14]. The objective function, $F(d,p)$, for the optimization was defined as follows:

$$F(d,p) = 1 - \frac{\int_{f_{\min}}^{f_{\max}} |R(d,p,f)|^2 \mathrm{d}f}{f_{\max} - f_{\min}} = 1 - \sum_{i=1}^{\mathrm{NF}} \left(\frac{|R(d,p,f_i)|^2}{\mathrm{NF}} \right) \tag{6}$$

The optimization function in Equation (6) is related to the average value of R^2 in the frequency range between $f_{\max}$ and $f_{\min}$. The integration is converted into a summation of the values of R^2/NF calculated at each evenly spaced frequency f_i of number NF in the prescribed frequency range.

Table 2. Double-layer absorber design results: thicknesses of pure E-glass fabric/epoxy laminates [NON] and thicknesses and filler contents of carbon nanomaterials in [CB], [CNF], and [CNT] laminates.

Material		Frequency range (GHz)	1st layer thickness (mm)	2nd layer thickness (mm)	2nd layer filler content (wt.%)
[NON]/[CB]	CASE 1	8.0–12.0	2.82	1.87	5.42
	CASE 2	7.0–13.0	2.82	2.03	5.16
	CASE 3	6.0–14.0	2.82	2.24	4.91
	CASE 4	5.0–15.0	2.83	2.51	4.64
	CASE 5	4.0–16.0	2.71	2.76	4.44
	CASE 6	8.0–14.0	2.56	1.81	5.32
	CASE 7	8.0–16.0	2.32	1.73	5.29
[NON]/[CNF]	CASE 1	8.0–12.0	2.98	1.20	2.69
	CASE 2	7.0–13.0	3.03	1.29	2.53
	CASE 3	6.0–14.0	3.02	1.48	2.17
	CASE 4	5.0–15.0	2.95	1.68	1.94
	CASE 5	4.0–16.0	2.83	1.83	1.79
	CASE 6	8.0–14.0	2.75	1.17	2.61
	CASE 7	8.0–16.0	2.48	1.17	2.44
[NON]/[CNT]	CASE 1	8.0–12.0	2.91	1.44	5.27
	CASE 2	7.0–13.0	2.90	1.56	5.05
	CASE 3	6.0–14.0	2.90	1.76	4.74
	CASE 4	5.0–15.0	2.85	1.97	4.50
	CASE 5	4.0–16.0	2.78	2.21	4.31
	CASE 6	8.0–14.0	2.63	1.41	5.13
	CASE 7	8.0–16.0	2.42	1.38	5.12

4. Results and discussion

4.1. Effect of variation in frequency range

The optimizations were performed over various frequency ranges. Table 2 displays the optimization results for several thicknesses of the two layers and filler content of the second layer. The various cases are distinguished by their f_{max} and f_{min}. Figure 4 presents the reflection losses of these design cases. In Figure 4, the double-layer absorbers have one or two peaks of reflection loss. In the double-peak cases, there are common regions of relatively low reflection loss between the two peaks and these regions create a broad absorbing bandwidth. In this situation, a very long distance between the two peaks allows for very low reflection loss between the peaks. Consequently, two peaks separated too far apart result in a deteriorated absorbance. Control of the distance between the two peaks, by choosing a proper frequency range, is required to obtain a good absorbance. All cases from CASE 1 to CASE 5 have a common center frequency of 10 GHz, which is the center frequency of the X-band. The thickness of the absorber increases proportionally to the frequency range. CASE 1,

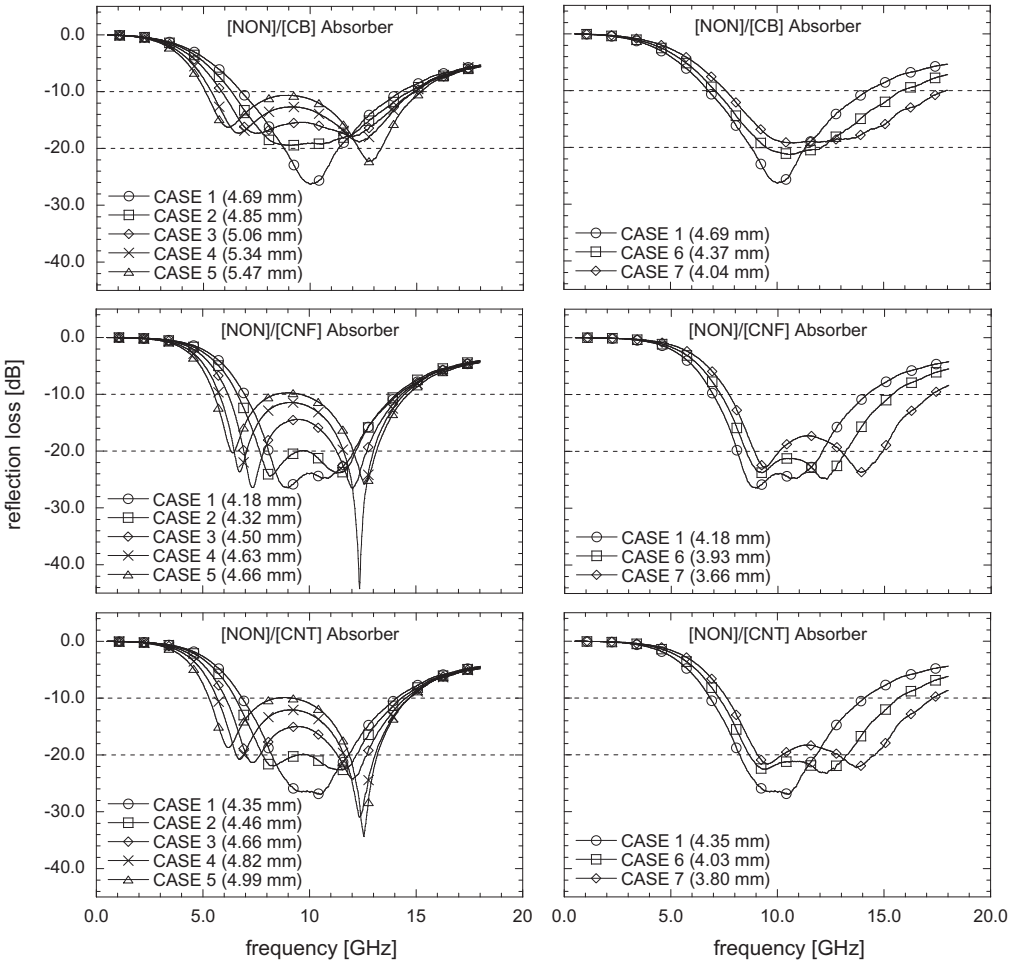

Figure 4. Reflection loss of optimally designed microwave absorbing composite laminates made of [NON]/[CB], [NON]/[CNF], and [NON]/[CNT] in different frequency ranges (see Table 2).

CASE 6, and CASE 7 all share the same f_{min}, however, the thickness of the absorbers decreases as the frequency range increases resulting in a broader absorbing bandwidth. From CASE 1 and CASE 2, the thickness of the absorber can be regarded as being dependent on the frequency of the first peak rather than the frequency range prescribed for the optimization.

It should be noted that the thickness of absorbers of [CB] is thicker than those of [CNF] and [CNT] in all cases. In addition, the peaks of the absorbers of [CB] are not easily separated and the reflection loss is quite low even when the peaks are sufficiently separated by using a large frequency range. Figure 5 is a comparison of the absorbers of [NON]/[CB], [NON]/[CNF], and [NON]/[CNT], which are all designed in the X-band (8.0–12.0 GHz). All the absorbers have a −10 dB bandwidth larger than 7.0 GHz and a −20 dB bandwidth more or less than 3.0 GHz. In Table 2, the thicknesses of [NON]/[CB], [NON]/[CNF], and [NON]/[CNT] are 4.69, 4.18, and 4.35 mm, respectively. Figure 6 shows the complex permittivity of

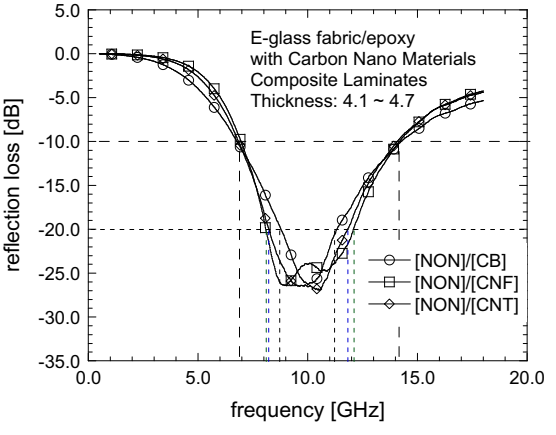

Figure 5. Reflection loss of absorbers designed for frequency range of 8.0–12.0 GHz (CASE 1 in Table 2).

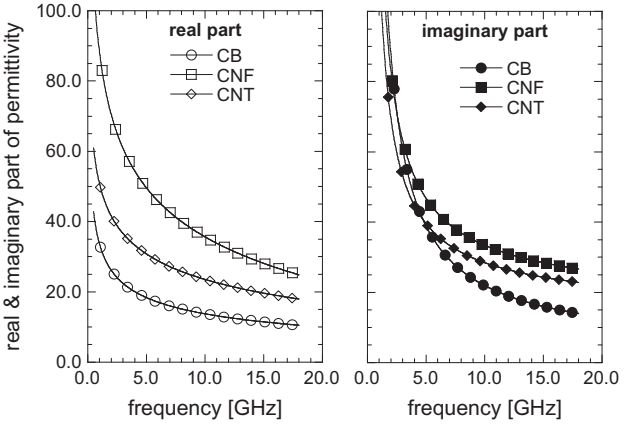

Figure 6. Complex permittivity for CB-, CNF-, and CNT-composites of absorbers designed for frequency range of 8.0–12.0 GHz (CASE 1 in Table 2).

CB-, CNF-, and CNT-composites for CASE 1, which are calculated by using the numerical model discussed in Section 3.2 [10]. In Figure 6, the real part of the complex permittivity displays a stronger dependence on the absorber thickness than the imaginary part does. This means that the real part of the complex permittivity is more important than the imaginary part in obtaining thinner layers and good peak separation for a large absorbing bandwidth in double-layer absorbers.

4.2. *Experimental verification*

To verify the performance of the absorbers in CASE 1, carbon nanocomposite laminates with filler content of 5.42 wt.% for CB-composites, 2.69 wt.% for CNF-composites, and 5.27 wt. % for CNT-composites were fabricated. To make the absorbers, the carbon nanocomposite prepregs were stacked on a 0.5 mm thick aluminum plate and cured in an autoclave. After cooling down the carbon nanocomposite/Al plate laminate, the pure glass/epoxy prepregs were stacked on the carbon nanocomposite/Al plate laminate and cured in the autoclave. Figure 7 shows the cross sectional configuration of the manufactured absorbers.

Figure 8 shows the results of both the measurement and the calculation of the complex permittivity of the carbon nanocomposite and the reflection loss for CASE 1. In Figure 8(a), the measured complex permittivity agrees quite well with the calculated result. To obtain optimal absorbers, the optimization process was repeated with the measured complex permittivity of the carbon nanocomposites. During this stage, the optimization variables were only the thicknesses of the first and second layers. The thickness of composite laminates can be determined by the normal ply thickness multiplied by the ply number. In this study, we determined the ply number from experiments based on the optimized thickness, as well as the accumulated data for the normal ply thickness obtained from the laminate thicknesses found in the complex permittivity measurements described in previous chapters. The normal ply thickness depends on the number of plies in addition to the amount and type of filler content of the carbon nanomaterials. Table 3 shows the ply thicknesses, ply numbers, and laminate thicknesses of the end products for the optimized CASE 1 absorbers.

In Figure 8(b), there is a small discrepancy between the calculated and the measured values, which is due to the difference in the layer thicknesses and the complex permittivity of

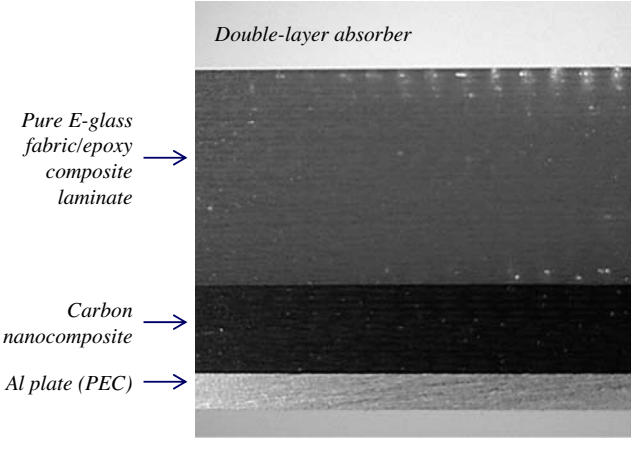

Figure 7. Cross-sectional configuration of double-layer microwave absorber.

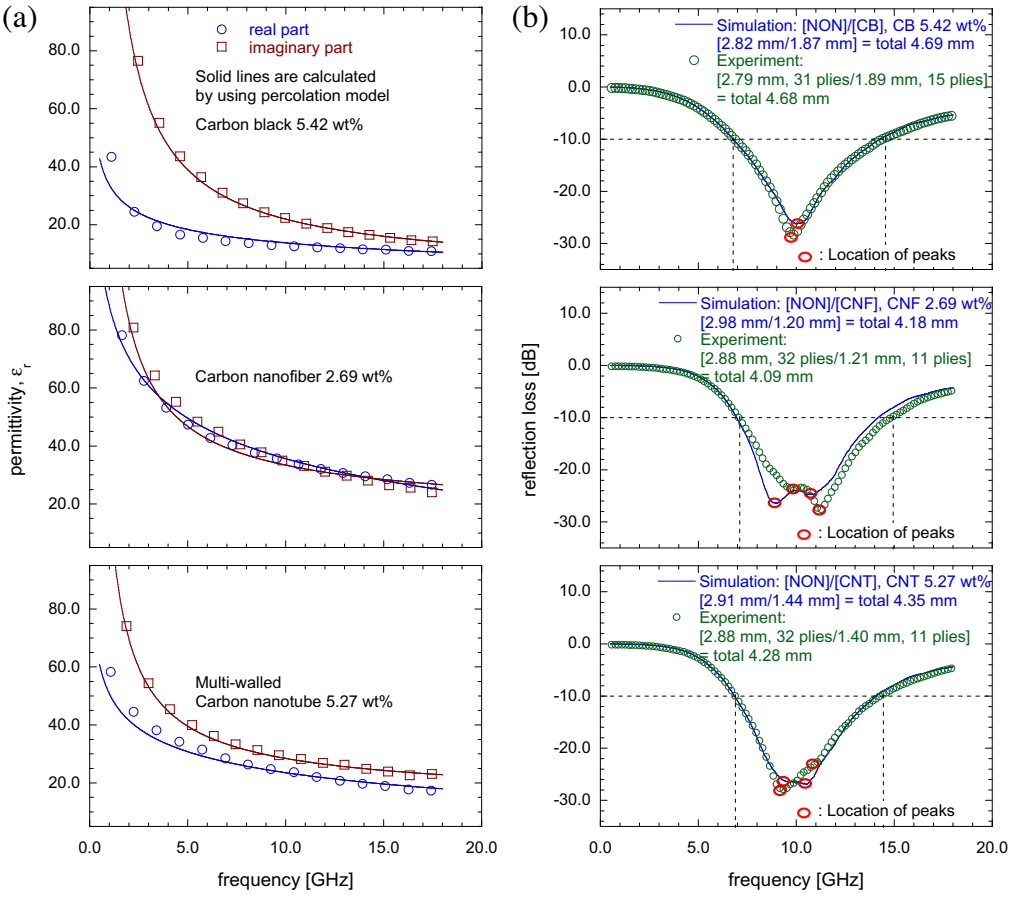

Figure 8. Comparison between simulated and measured results of (a) complex permittivity of CB-, CNF-, and CNT-composites and (b) reflection loss designed for frequency range of 8.0–12.0 GHz (CASE 1 in Table 2).

the second layer between the optimal design and the real product, as well as the scatter in the measurement of the electromagnetic properties. Table 3 shows the absorber thickness, −10 dB bandwidth, and −20 dB bandwidth of each absorber. The order of the thickness of the absorbers is CB > CNT > CNF, but the order of their absorbing bandwidth is CNF > CNT > CB.

Table 3. Properties of absorbers manufactured using optimal design results of double-layer absorbers in X-band (8.0–12 GHz): ply thicknesses, ply numbers, and laminate thicknesses.

Material		Filler content (wt.%)	Ply thickness (mm)	Ply number	Laminate thickness (mm)
[NON]/[CB]	NON	0	0.090	31	2.790
	CB	5.42	0.126	15	1.890
[NON]/[CNF]	NON	0	0.090	32	2.880
	CNF	2.69	0.110	11	1.210
[NON]/[CNT]	NON	0	0.090	32	2.880
	CNT	5.27	0.127	11	1.397

Table 4. Thickness and absorbing bandwidth of each double-layer absorber.

Material	Thickness of absorbers (mm)	10-dB Absorbing bandwidth (GHz)	20-dB Absorbing bandwidth (GHz)
[NON]/[CB]	4.680	7.5 (6.9–14.4)	2.6 (8.7–11.3)
[NON]/[CNF]	4.090	7.7 (7.1–14.8)	3.8 (8.7–12.5)
[NON]/[CNT]	4.277	7.4 (6.9–14.3)	3.3 (8.3–11.6)

5. Conclusion

Double-layer microwave absorbers made of E-glass/epoxy composite laminates containing carbon black, carbon nanofibers, and carbon nanotubes were designed using a genetic algorithm, and a numerical model for the complex permittivity of carbon nanocomposites, as proposed by Kim et al. [10], was used. The first layer of the absorbers was pure E-glass/epoxy composite laminates and the second layer was carbon nanocomposites laminates containing CB, CNF, and CNT. Double-layer absorbers with a broad bandwidth were realized by obtaining two peaks in the frequency domain (i.e. same number of peaks as the number of layers in the absorber) under the condition that the distance between the two peaks was suitable to allow a moderate reflection loss. The distance between the two peaks could be controlled by optimizing the thicknesses of the two layers and the filler content of the second layer. The optimal values were obtained by employing the appropriate frequency range in the design process.

When the prescribed frequency range was in the X-band (8.0–12.0 GHz), the absorber composed of the CB-composite had an obscure separation of the peaks. However, the absorbers composed of CNF- and CNT-composites showed an obvious peak separation, even though the total thickness of the absorber of the CB-composite was much larger than that of the CNF- and CNT-composites. Consequently, the absorber made of the CB-composite had a narrower bandwidth than the absorbers made of the CNF- and CNT-composites. The large real part of the complex permittivity is more important than the imaginary part to obtain thin layers and good peak separation for a large absorbing bandwidth. Owing to the large real part of the complex permittivity of the CNF- and CNT-composites, the 10-dB bandwidth and the thickness of their absorbers were 7.7 GHz and 4.090 mm and 7.4 GHz and 4.277 mm, respectively. The 10-dB bandwidth and absorber thickness for the CB-composite were 7.5 GHz and 4.680 mm, respectively.

Acknowledgment

This work was supported by New & Renewable Energy R&D Program (2008-N-WD08-P-02) under the Korea Ministry of Knowledge Economy (MKE).

References

[1] Stonier RA. Stealth aircraft & technology from World War II to the Gulf, part I: history and background. SAMPE J. 1991;27:9–17.
[2] Stonier RA. Stealth aircraft & technology from World War II to the Gulf, Part II: Applications and Design. SAMPE J. 1991;27:9–18.
[3] Bryanton M, Pinto J, Matthews J, Sarno C, Moore Z, Bellanger Y, Brown T, Rashid L, Chambers B, Ford L, Tennant A. Stealth technology for wind turbines. (UK): BERR; 2007 (No. TES101865).
[4] Oh J-H, Oh K-S, Kim C-G, Hong C-S. Design of radar absorbing structures using glass/epoxy composite containing carbon black in X-band frequency ranges. Comp. Part B. 2004;35:49–56.
[5] Jung W-K, Kim B-K, Won M-S, Ahn S-H. Fabrication of radar absorbing structure (RAS) using GFR-nano composite and spring-back compensation of hybrid composite RAS shells. Compos. Struct. 2006;75:571–576.

[6] Lee S-E, Kang J-H, Kim C-G. Fabrication and design of multi-layered radar absorbing structures of MWNT-filled glass/epoxy plain-weave composites. Compos. Struct. 2006;76:397–405.
[7] Park K-Y, Lee S-E, Kim C-G, Han J-H. Fabrication and electromagnetic characteristics of electromagnetic wave absorbing sandwich structures. Compos. Sci. Technol. 2006;66:576–584.
[8] Chin W-S, Lee D-G. Development of the composite RAS (radar absorbing structure) for the X-band frequency range. Compos. Struct. 2007;77:457–465.
[9] Kim J-B, Lee S-K, Kim C-G. Comparison study on the effect of carbon nano materials for single-layer microwave absorbers in X-band. Compos. Sci. Technol. 2008;68:2909–2916.
[10] Kim J-B, Kim C-G. Study on the semi-empirical model for the complex permittivity of carbon nanocomposite laminates in microwave frequency band. Compos. Sci. Technol. 2010;70:1748–1754.
[11] Pesque JJ, Bouche DP, Mittra R. Optimization of multilayer antireflection coatings using an optimal control method. IEEE Trans. Microwave theory Tech. 1992;40:1789–1796.
[12] Michielssen E, Sajer J-M, Ranjithan S, Mittra R. Design of lightweight, broad-band microwave absorbers using genetic algorithm. IEEE Trans. Microwave theory Tech. 1993;41:1024–1031.
[13] Perini J, Cohen LS. Design of broad-band radar-absorbing materials for large angles of incidence. IEEE Trans. Electromagn. Compat. 1993;35:223–230.
[14] Weile DS, Michielssen E, Goldberg DE. Genetic algorithm design of pareto optimal broadband microwave absorbers. IEEE Trans. Electromagn. Compat. 1996;38:518–525.
[15] Cao M, Zhu J, Yuan J, Zhang T, Peng Z, Gao Z, et al. Computation design and performance prediction towards a multi-layer microwave absorber. Mater. Des. 2002;23:557–564.
[16] Goudos SK. A versatile software tool for microwave planar radar absorbing materials design using global optimization algorithms. Mater. Des. 2007;28:2585–2595.
[17] Goldberg DE. Genetic algorithm in search, optimization, and machine learning. Boston (MA): Addison-Wesley; 1989.